



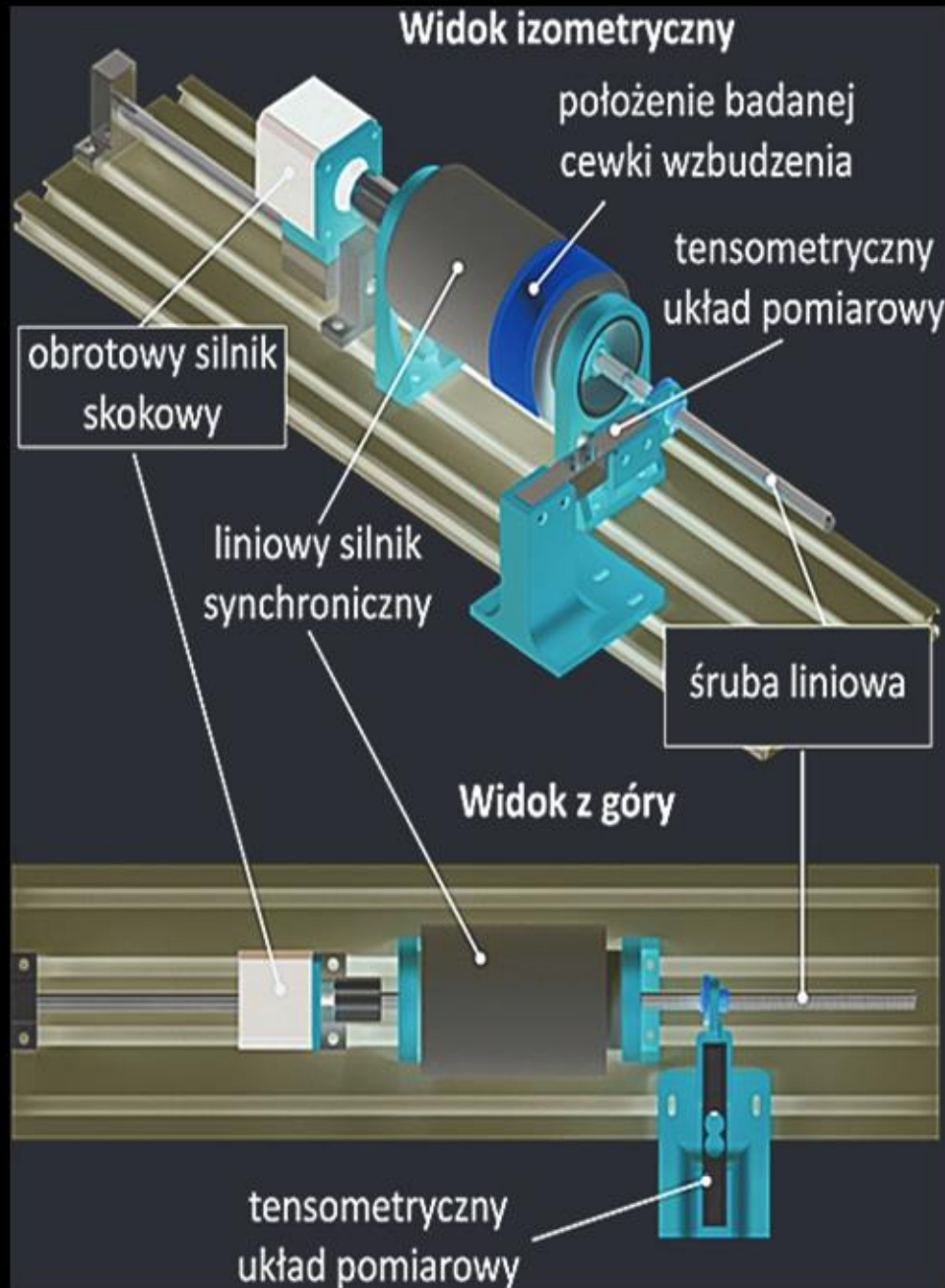
PRZEGŁĄD ELEKTROTECHNICZNY

ROK 100

WYDAWNICTWO
SIGMA-NOT



cena 85 zł
(w tym 8% VAT)



Test sstand for determinning the distribution of
electromagnetic force acting in a linear cylindrical
synchronous motor – page 50

PRZEGŁĄD ELEKTROTECHNICZNY Vol 2024, Nr 2

Spis treści

01	Abdalrhman Adel, Osama A. Omer , M. Alamir, M. Anwar, C. Qunsheng, Amir Almslmany- Projekt unikalnego systemu optycznego i wdrożenie systemu rentgenowskiego do badań nieniszczących rakiet na paliwo stałe	1
02	Abdallah BELABBES, Anouar LAIDANI, Amina YACHIR, Allal El Moubarek BOUZID, Riyadh BOUDDOU, Omar Abdelaziz LITIM - Zaawansowane sterowanie systemem konwersji energii wiatrowej opartym na PMSG przy użyciu modelu predykcyjnego i sterowania w trybie ślizgowym	10
03	Islam M. Ibrahim, Nada I. Farah, Mohamed I. Ahmed, Hala M Abdelkader, Ahmed Jamal Abdullah Al-Gburi, Zahrialadha Zakaria, Rania H. Elabd, M. M. Elsherbini - Złożona macierz układów anten Mm-Wave do zastosowań 5G	17
04	Ahmed Nour El Islam AYAD, *Houari BOUDJELLA, Wafa KRIKA, Ilies REZZAG BARA, Benyekhlef LAROUCI - Symulacja drzew elektrycznych rosnących w trójżyłowym kablu podmorskim	23
05	Hiba-Allah T. Abdullah, Riyadh Zaghloul Mahmood, Sanabel M. Alhaj Zber, Rasha A.Mohammed, Marwa Riyadh Ahmed, Azhar W. Talab - Implementacja algorytmów wykrywania trzech krawędzi opartych na FPGA (Sobel, Prewitt i Roberts) do przetwarzania obrazu	29
06	Małgorzata ŁATKA - Analiza wybranych parametrów jakości energii elektrycznej w miejskich i rejonowych sieciach elektroenergetycznych niskiego napięcia z udziałem generacji rozproszonej na wybranym obszarze	34
07	Mirosław WCIŚLIK, Robert KAZAŁA - Analiza symulacyjna symetrycznego trójfazowego obwodu prądu przemiennego z obciążeniem nielinijnym	38
08	Mirosław PAROL - Mikrosieci – mikrosystemy energetyczne zasilające odbiorców energii. Stan aktualny i perspektywy rozwoju	44
09	Sebastian BARTEL, Krzysztof KLUSCZYŃSKI, Zbigniew PILCH - Stanowisko badawcze do wyznaczania rozkładu siły elektromagnetycznej działającej w liniowym cylindrycznym silniku synchronicznym z magnesem trwałym	50
10	Sebastian BARTEL, Krzysztof KLUSCZYŃSKI - Zagadnienie doboru proporcji geometrycznych cewek wzbudzenia w liniowym cylindrycznym silniku synchronicznym z magnesem trwałym jako biegkiem	55
11	Stanisław CZAPP - Wyłączniki różnicowoprądowe w instalacjach ładowania pojazdów elektrycznych	62
12	Wiktoria GRYCAN – Wsparcie legislacyjne dla energetyki prosumenckiej w ramach bezpieczeństwa elektrycznego sieci elektroenergetycznej	66
13	Marek JAWORSKI - Wpływ konstrukcji słupów oraz układu faz na rozkłady pola elektrycznego i magnetycznego w otoczeniu linii 400 kV	70
14	Jakub Beling, Dorota Rabczuk - Dobór filtrów cyfrowych w pomiarach sygnałów fotopletyzmograficznych	74
15	Sylwia BERDOWSKA - Analiza potencjału wytwarzania energii elektrycznej w instalacji komina słonecznego z nachylonym kolektorem słonecznym	78
16	Machmud Effendy, Dandy Dwi Saputra, Fourys Yudo Setiawan Paisey - Analiza przepływu mocy generacji rozproszonej i rozproszonej pamięci masowej (DGDC) w mikrosieci prądu stałego przy użyciu metody Newtona Raphsona	84
17	Artur BUGAŁA, Antoni ARENDACZ, Dorota BUGAŁ - Analiza wydajności dwustronnego modułu fotowoltaicznego pracującego w standardowej i dedykowanej konstrukcji wsporczy	87
18	Hari Agus Sujono, Achmad Saiful Faris - Projekt detektora świeżeści wołowiny na podstawie koloru i zapachu metodą rozmytą Mamdani	92
19	Keltoum MOURADJ , Mustapha KHELIFI, Abdesselam BASSOU, Mohamed Rida LAHCENE - Poprawa QoS dla systemu 5G przy użyciu kodera UTTCM przez kanał EPA	97
20	Ahmad BOUSSOUFA, Aimad AHRICHE, Madjid KIDOUCHE, Mohammed Zinelabidine DOGHMANE - Wpływ kolejności dyskretyzacji na rozszerzoną estymację filtra Kalmana dla generatora indukcyjnego z podwójnym zasilaniem	102
21	Abderrahim ZEMMIT, Sabir MESSALTI, Abdelghafour HERIZI - Nowa bezpośrednia kontrola momentu obrotowego silnika indukcyjnego z podwójną gwiazdą przy użyciu techniki optymalizacji Gray Wol	109
22	Nur HAMZAH, Suryanto SURYANTO, Muhammad ANSHAR, Firman FIRMAN, Muhammad Ruswandi DJALAL, Muhammad Alif AL AFGAN - Modelowanie termodynamiczne elektrowni przetwarzającej odpady na energię: studium przypadku w mieście Makassar w Indonezji	114
23	Vadim MANUSOV, Alifbek KIRGIZOV, Murodbek SAFARALIEV, Inga ZICMANE, Svetlana BERYOZKINA, Sherkhon SULTONOV - Stochastyczna metoda przewidywania wydajności energii elektrycznej odbieranej z panelu słonecznego	118
24	Oleksandr Sinyavsky, Vitaliy Savchenko, Andrii Nesvidomin, Vasyl Bunko, Vasyl Ramsh, Mykola Potapenko - Wpływ jakości energii elektrycznej na charakterystyki energetyczne maszyn rolniczych	123
25	Benmebarek, L. Alloui, Y. Gabi, S. M. Mimoune, B. Wolter - Trójwymiarowe modelowanie numeryczne układu prądów wirowych przy użyciu metody objętości skończonych	127
26	Ilham RAHIMLI, Aliashraf BAKHTIYAROV, Gulshan ABDULLAYEVA, Sona RZAYEVA - Zastosowanie optycznych czujników prądu w podstacjach elektrycznych	132
27	Ilkin Marufov , Najiba Piriyeva, Nijat Mammadov, Shukufa Ismayilova⁴ - Obliczanie parametrów lewitacji indukcyjnej w osi pionowej układu generator wiatrowy-turbina, lewitacji i pętli wpływów	135
28	Andi Abdul Halik LATEKO, Yusri Syam AKIL - Analiza VECM dotycząca wpływu wzrostu gospodarczego i inwestycji na zużycie energii elektrycznej w Indonezji	140

PRZEGŁĄD ELEKTROTECHNICZNY Vol 2024, Nr 2

Spis treści

29	Angati Kalyan KUMAR, Tsehay Admassu ASSEGIE, Ayodeji Olalekan SALAU, Komal Kumar NAPA, Suguna R - Funkcja przyczyniająca się do dogłębniego zrozumienia interpretacji modelu uczenia maszynowego	145
30	Mustafa HAMIDOV, Elbrus AHMEDOV, Hamida HAMDOVA, Sona RZAYEVA⁴ - Analiza i opracowanie modelu matematycznego metody akustycznej monitorowania parametrów odwierturnego procesu wiertniczego	149
31	Anatolii SEMENOV, Stanislav POPOV, Serhii YAKHIN, Bauyrzhan YELEUSSINOV, Tamara SAKHNO¹- Ocena niebezpieczeństwa stosowania lamp ultrafioletowych w instalacjach elektrycznych	152
32	Hryhorii KALETNIK, Vitalii YAROPUD, Yurii POLIEVODA, Olena SOLONA, Ihor BABYN, Ihor TVERDOKHLIB - Badanie procesu suszenia aktywno-wentylacyjnego produktów przetwórstwa frakcyjnego traw strączkowych	156
33	Nataliia LUTSKA, Nataliia ZAIETS, Lidia VLASENKO - Opracowanie Systemu Diagnostyki Stanu Napędów Elektrycznych Przedsiębiorstwa Spożywczego	164
34	Muhammad Tajammal Chughtai - Zbieranie napięcia za pomocą struktur dzianych	168
35	Hafizudin Fikri KHAIRUDIN, Suziana AHMAD, Mohd Zaidi Mohd TUMARI, Amirul Syafiq SADUN, Izadora MUSTAFFA¹- Robot do czyszczenia powierzchni wody oparty na IoT z transmisją na żywo	172
36	Siti Fatimah SULAIMAN, Nurul Aini NGATENI, Khairuddin OSMAN, Sharatul Izah SAMSUDIN, Noor Asyikin SULAIMAN, Noorhazirah SUNAR - Modelowanie i rozwój sterownika predykcyjnego do sterowania pozycjonowaniem układu silownika elektrohydraulicznego (EHA)	177
37	Wittawat WASUSATHIEN, Chanchai THONGSOPA, Samran SANTALUNAI, Thanaset THOSDEEKORAPHAT, Nuchanart SANTALUNAI - Pomiar właściwości dielektrycznych mieszanin różnych odmian ryżu w celu wykrywania zanieczyszczeń w przemyśle	182
38	Sabir BAGHIROV, Yulia BASOVA, Liudmyla GUBA, Hryhorii KOZHUSHKO - Przewidywanie żywotności lamp LED na podstawie ekstrapolacji współczynnika zachowania strumienia światelnego r	190
39	Saad Alhamid, Omar hamandouch, Ahmed Haj Darwish - Hybrydowy algorytm pszczoły poprawiający wydajność systemów dystrybucji promieniowej	193
40	Antoni Różowicz, Mariusz Deląg - Promieniowanie rezonansowe UV w funkcji częstotliwości prądu w obwodzie lamp oraz warunków środowiska pracy	197
41	Sebastian Różowicz, Mariusz Deląg - Projektowanie oraz testy na zgodność z regulaminem 65 na przykładzie specjalnej lampy ostrzegawczej	200
42	Piotr Jankowski, Damian Hallmann - Symulacyjne badanie właściwości dynamiczno-termicznych ultra-szybkiego napędu indukcyjno-dynamicznego	203
43	Maciej WŁODARCZYK, Andrzej ZAWADZKI, Sebastian RÓŻOWICZ - Analiza możliwości rozszerzenia metod trzech rzędnych i zastosowania do elementów nieliniowych z histerezą	209
44	Sebastian RÓŻOWICZ, Maciej WŁODARCZYK, Andrzej ZAWADZKI¹- Pewne uwagi o symetrii czwórników pasywnych w stanach ustalonych i nieustalonych	214
45	Marcin POŁOMSKI, Tomasz KRASZEWSKI, Artur PASIERBEK, Anna PIWOWAR, Magdalena KRASZEWSKA - Metoda skanowania z użyciem światła strukturalnego w procesie identyfikacji wad detali	217
46	KAZIMIERZ KAWA, RAFAŁ MULARCZYK, WALDEMAR BAUER, EDYTA KUCHARSKA - Wpływ czynników zewnętrznych na predykcję zużycia energii elektrycznej w budynku biurowym z panelami fotowoltaicznymi	221
47	Daniel ZEJLER, Piotr ZIENTEK²- Czujniki specjalne w zastosowaniach systemów sygnalizacji pożaru	227
48	Tomasz Kossowski, Paweł Szczupak - Analiza rozkładu pola elektrycznego w kondensatorze płytowym, równoległym przeznaczonym do badania odporności urządzeń elektrycznych na piorunowy impuls elektromagnetyczny	232
49	Piotr Warda - Metoda dynamicznego doboru częstotliwości zegarowej w przetworniku częstotliwość-kod	235
50	Jacek KOZYRA, Zbigniew ŁUKASIK, Aldona KUŚMIŃSKA-FIJAŁKOWSKA - Analiza wybranych aspektów zdolności przesyłowej dla zastąpienia linii napowietrznej linią kablow	241
51	Ayoob Alateeq - Projekt trój fazowego falownika wielopoziomowego wykorzystującego ogniwo SC do zastosowań fotowoltaicznych	248
52	Majid H. ABDULLAH, Petar BIŠEVAC, Ratko IVKOVIĆ, Petar SPALEVIĆ, Srđan Milosavljević - Wykorzystanie sztucznej inteligencji do segmentacji tekstu z obrazów	255
53	T Praveen Kumarar, S Ganapathy, M Manikandan - Analiza stabilności napięcia dla systemu fotowoltaicznego podłączonego do sieci przy użyciu zoptymalizowanego sterowania w oparciu o ANFIS IOT	259
54	Titiek Suheta, Syahri Muharom, Misbahul Munir - Analiza monokrystalicznych i polikrystalicznych paneli słonecznych w małych systemach wytwarzania energii opartych na mikrokontrolerach	267
55	Abdelhalim Ghediri, Noureddine Goléa - Wykrywanie awarii silników indukcyjnych za pomocą analizy sygnału prądu silnika (MCSA) i dwuetapowego klasyfikatora maszyny wektorów nośnych (SVM)	272
56	Taha RACHDI, Yahia SAOUDI, Larbi CHRIFI-ALAOUI, Ayachi ERRACHDI - Zwiększenie wydajności inteligentnych sieci poprzez optymalne rozmieszczenie FAKTÓW: przypadek TCSC	279
57	Irena DROFOVA, Martin HROMADA, Milan ADAMEK, Jan VALOUCH, Pavel WANECKI - Urządzenia skanujące 360° do rekonstrukcji cyfrowych bliźniaków 3D	286
58	Hemza Medoukali, Boubakeur Zegnini, Mossadek Guibadj - Badanie wpływu napięcia stałego na zjawisko drzewa elektrycznego w materiałach izolacyjnych XLPE	290
59	Damian BURZYŃSKI, Leszek KASPRZYK - Model predykcyjny stanu dostępnej energii ogniw litowo-żelazowo-fosforanowych	294

Study of the process of active-ventilation drying of legume grasses' fractional processing products

Abstract. Based on the results of research, the technological and constructive-technological scheme of the conveyor heat-mass exchange equipment for the fractional processing of leguminous herbs is substantiated, which is made in the form of a chamber with horizontal belt conveyors installed in it, in the middle of which are placed calorifiers with heated steam, and centrifugal fans are installed on top of the chamber. Based on the results of analytical studies, the design and technological parameters of the developed conveyor heat-mass exchange equipment for the fractional processing of legumes were calculated. It was established that the productivity of the wet product is 1300 kg/h. The product comes out of the dryer at a humidity of 7% and a temperature of 45 °C. Based on the results of the calculation, we obtained the design parameters of the working area of the conveyor heat and mass exchange equipment: length – 3.8 m, width – 2.1 m and height 2.3 m. Total heat loss in the drying unit – 13 kJ/kg. The speed of the belt conveyor is 0.11 m/s. Using the Simcenter STAR-CCM+ software package, a simulation of the technological process of drying in the developed conveyor heat and mass exchange equipment was carried out. Visualizations of the flow rate distribution of particles of products of fractional processing of legumes and air flow in the area of the conveyor heat and mass exchange equipment were obtained in scalar and vector form. The temperature distribution of the air flow in the area of the conveyor heat and mass exchange equipment was determined in a scalar form and its influence on the temperature of the particles of the fractional processing of leguminous grasses moving along belt conveyors was revealed. The presented results of numerical modeling confirm the analytical calculations. However, in the future, it is necessary to carry out experimental studies of the drying process of products of fractional processing of leguminous herbs and empirically check the rational structural and technological parameters of the conveyor heat and mass exchange equipment.

Streszczenie. Na podstawie wyników badań uzasadniono schemat technologiczny i konstrukcyjno-technologiczny przenośnikowego urządzenia wymiany ciepła i masy do frakcyjnej obróbki ziół roślin strączkowych, który wykonany jest w postaci komory zainstalowanymi w niej poziomymi przenośnikami taśmowymi, w pośrodku których umieszczone są podgrzewacze z podgrzaną parą, a na górze komory zainstalowane są wentylatory odśrodkowe. Na podstawie wyników badań analitycznych obliczono konstrukcję i parametry technologiczne opracowanego przenośnikowego urządzenia wymiany ciepła i masy do frakcyjnej obróbki roślin strączkowych. Ustalono, że wydajność mokrego produktu wynosi 1300 kg/h. Produkt wychodzi z suszarki przy wilgotności 7% i temperaturze 45 °C. Na podstawie wyników obliczeń uzyskano parametry projektowe powierzchni roboczej przenośnika urządzeń wymiany ciepła i masy: długość – 3,8 m, szerokość – 2,1 m i wysokość 2,3 m. Sumaryczna strata ciepła w zespole suszarni – 13 kJ/kg. Prędkość przenośnika taśmowego wynosi 0,11 m/s. Wykorzystując pakiet oprogramowania Simcenter STAR-CCM+ przeprowadzono symulację procesu technologicznego suszenia w opracowanym przenośnikowym urządzeniu do wymiany ciepła i masy. Wizualizacje rozkładu natężenia przepływu cząstek obróbki frakcyjnej ziół strączkowych oraz przepływu powietrza w obszarze urządzeń wymiany ciepła i masy przenośnika uzyskano w postaci skalarnej i wektorowej. Wyznaczono w postaci skalarnej rozkład temperatury strumienia powietrza w obszarze urządzeń wymiany ciepła i masy przenośnika oraz ujawniono jego wpływ na temperaturę cząstek obróbki frakcyjnej traw strączkowych poruszających się wzduż przenośników taśmowych. Przedstawione wyniki modelowania numerycznego potwierdzają obliczenia analityczne. Jednak w przyszłości konieczne jest przeprowadzenie badań doświadczalnych procesu suszenia produktów obróbki frakcyjnej ziół strączkowych oraz empiryczne sprawdzenie racjonalnych parametrów konstrukcyjnych i technologicznych urządzeń wymiany ciepła i masy przenośnika. (Badanie procesu suszenia aktywno-wentylacyjnego produktów przetwórstwa frakcyjnego traw strączkowych)

Keywords: drying, structural and technological scheme, heat and mass exchange equipment, dryer, alfalfa, calculation, simulation, parameters
Słowa kluczowe: suszarnia, schemat konstrukcyjny i technologiczny, urządzenia do wymiany ciepła i masy, suszarnia, lucerna, obliczenia,

Introduction

Nowadays, an important task in the agricultural industry is to ensure adequate nutrition for farm animals. A rational approach to this task is to use available and cheap local plant raw materials [1, 2]. As a source of vegetable protein, carotene and vitamins, which allows to reduce the use of expensive protein raw materials, such as soybean meal, fish meal and others, forage grasses are widely used, in particular, alfalfa, clover, dogwood and safflower. Among them, a special place is occupied by seed alfalfa (*Medicago sativa L.*), which contains 17–19% protein and up to 200 mg/kg of carotene in leaves and stems [3-5].

One of the disadvantages of alfalfa as a feed raw material is the high initial humidity (from 50% to 80%), which makes it difficult to store it for a long time [6]. Therefore, the mass of alfalfa leaves is dried to a moisture content of 7-15%. The traditional method of natural drying of alfalfa to obtain hay is becoming less and less popular due to the length of the process and low productivity [7]. Instead, intensive drying technology, which includes washing the alfalfa leaf mass, high-temperature convective drying, and granulation, is becoming increasingly common [8]. However, the disadvantage of this technology is a significant decrease in the content of carotene and vitamins

due to high temperature [9]. This drawback is also typical for convective drying of other plants. In addition, due to the low thermal conductivity of green plants, including alfalfa, convective drying has a significant duration, which negatively affects the preservation of carotene and other food substances [10]. At the final stage of drying, when the moisture content of the plant material is significantly reduced, its thermal conductivity and electrical conductivity decrease even more, which leads to an increase in energy consumption for the process.

In studies [11], the following drying methods were used for alfalfa: drying in the field to 50% dry matter and finishing drying in a ventilated warehouse; drying in field conditions without turning over; drying with only one flip and drying with two flips. The best result was shown by the inversion drying method.

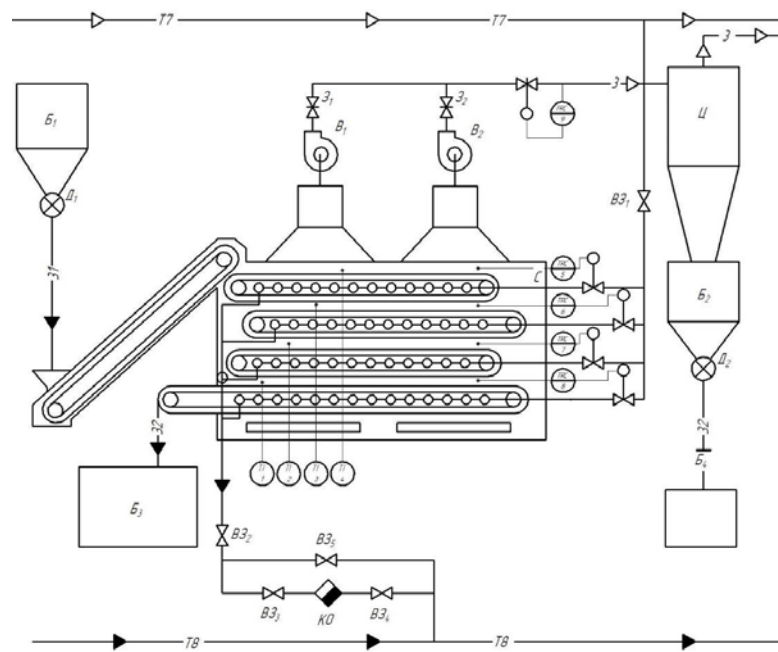
In studies [12–17] many different means for drying alfalfa were considered. According to their design, they can be divided into the following groups: chamber, drum, tunnel, shaft and belt dryers. Belt dryers are of greatest interest, as they operate continuously, which ensures drying efficiency in the overall technological line of processing alfalfa into fodder.

Analytical studies

Fig. 1 shows the process flow diagram of conveyor-type equipment meant for heat and mass exchange of legume grasses' fractional processing products. The product are dried via moisture return by heat carrier product with air being used as such product.

The wet products of legume grasses' (lucerne) fractional processing, with the moisture content of $W_n = 50\%$ and bunker B_1 temperature of $\theta_1 = 17.6^\circ\text{C}$ enters an inclined conveyor, which feeds the product into drying chamber C. In the drying chamber, the product moves on belts. Air at

the initial temperature $t_0 = 17.6^\circ\text{C}$ with the relative humidity of $\phi_0 = 78\%$ is pumped by centrifugal fans B_1 and B_2 into the drying chamber. The air is heated step by step in the heaters installed between the working and idle branches of the belts due to condensation of steam that heats and has the temperature of $t_{ha} = 140^\circ\text{C}$ at the pressure of $P_{ha} = 0.4 \text{ MPa}$. The product is dried to the moisture content of $W_k = 7\%$. Dried products enter bunker B_3 . Exhaust air enters LH-15 cyclone, where it is cleaned of small particles and released into the atmosphere. Dried products from the cyclone enter bunker B_2 .



C – drying chamber; LH – cyclone; B_{1-2} – fan; B_{3-4} – bunker; D_{1-2} – dispenser; KO – condensate trap; $B3_{1-5}$ – shut-off valve; $B3_{1-2}$ – locking bar; 31–31 – initial product; 32–32 – dried product; 3–3 – air; T7–T7 – steam; T8–T8 – condensate; TRC - automatic temperature control; FRC - automatic throughput regulation

Fig. 1. Process flow diagram of conveyor-type heat and mass exchange equipment (dryer)

Fig. 2 shows conveyor-type heat and mass exchange equipment (dryer). The dryer represents a chamber closed by metal shields and doors. There are two exhaust devices in the heat and mass exchange equipment. The supporting part of the dryer is represented by the bed, inside which there are five pairs of drums of 246 mm diameter. Each pair carries an endless mesh-type stainless steel wire band. One of the drums in each pair is a leading one, the other being tension-type. Scrapers installed on the drums are used to clean the drums from stuck-on product. The inclined conveyor installed at the angle of 40° to the horizon is used to feed the product to the dryer. Sections of steam heaters are located in the space between the branches of each conveyor. Under the pressure of 0.4 Mpa, steam is supplied to the heater. The exhaust device has two chambers and two fans. The fans' performance is regulated by the valve installed in the upper part of the exhaust chamber. Air is taken from the room through movable curtains of the dryer's lower part. The product is fed by the inclined conveyor to the upper working belt of the dryer, then to the second, third and further ones, passing successively through five belts. Passing through the product layer, air preheated in the heaters absorbs moisture and is discharged from the dryer. At the end of the fourth belt in the heat and mass exchange equipment, a tray for unloading or the next conveyor is available

From the equation of the drying unit's material balance, we determine the consumption of moisture W , which is removed from the material being dried [18]:

$$(1) \quad W = G_H \cdot \frac{W_H - W_K}{100 - W_K},$$

where G_H is the productivity of the dry matter unit, kg/h; W_H – the product's initial moisture content, %; W_K is the product's final moisture content, %.

The dryer's output of dry material

$$(2) \quad G_K = G_H - W,$$

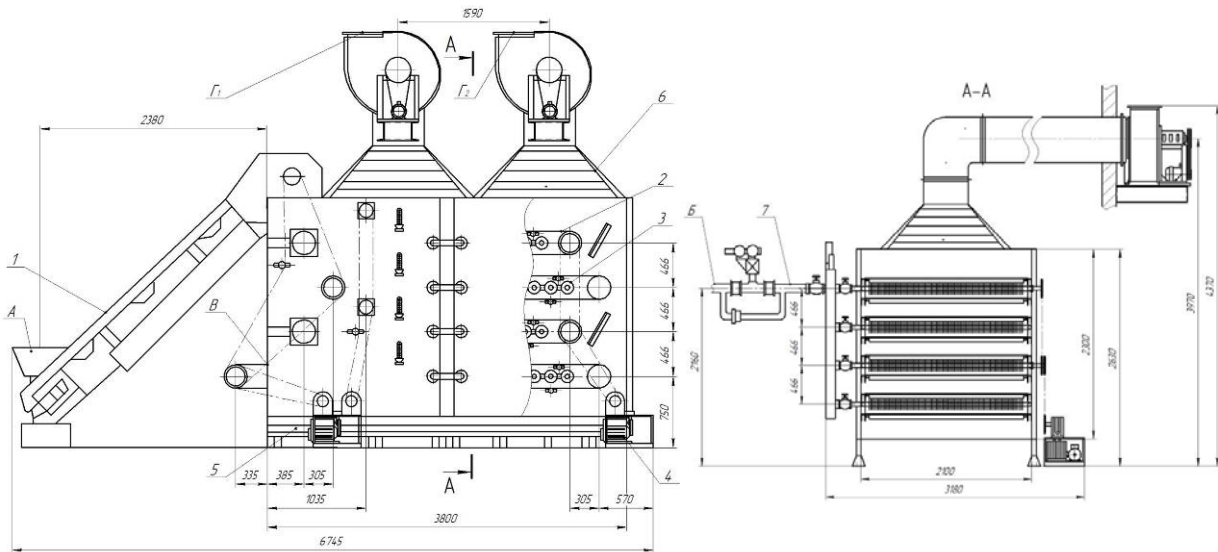
Let us assume that for the four belts installed, the amount of moisture that evaporates on belt 1 is 15%, on belt 2 – 30%, on belt 3 – 30%, on belt 4 – 25% amounts to $W_1 = 81.77 \text{ kg/h}$, $W_2 = 163.65 \text{ kg/h}$, $W_3 = 163.65 \text{ kg/h}$ and $W_4 = 136.29 \text{ kg/h}$.

Based on known temperature and relative humidity, the specific moisture content is calculated using formula [14]:

$$(3) \quad x = \kappa \cdot \frac{\phi \cdot P_H}{B - \phi \cdot P_H},$$

where $\kappa = 0.622$ is the ratio of molar masses of water vapor and air; P_H is the pressure of saturated water vapor at a given air temperature, Pa; B is the barometric air pressure, Pa; ϕ is air humidity.

According to the calculation results, specific moisture content at the entrance to the heater is $9.99 \cdot 10^{-3} \text{ kg/kg}$.



1 – inclined belt conveyor; 2 – belt conveyor; 3 – heating battery; 4 – drive; 5 – bed; 6 – exhaust device; 7 – steam pipeline; A – input of wet material; B – steam inlet; Γ_{1-2} – exhaust air outlet
Fig. 2. Structural diagram of the conveyor heat and mass exchange equipment

Since air is heated in the heater at constant air moisture content, the absolute air humidity at the entrance to the heater is the same as at the entrance to the dryer – $9,99 \cdot 10^{-3} \text{ kg/kg}$.

Using formula (3), specific moisture content at the exit from the dryer was calculated – 0.0305 kg/kg .

The enthalpy of moist air is the sum of the enthalpies of dry air and water vapor per 1 kg of dry air [16, 18]:

$$(4) \quad I = C_{c,n} \cdot t + x \cdot i_n ,$$

where $C_{c,n}$ – average specific heat capacity of dry air, $\text{kJ}/(\text{kg.K})$; t – temperature of moist air, $^{\circ}\text{C}$; x – specific moisture content, kg/kg c.n.; i_n – specific enthalpy of superheated steam, kJ/kg

$$(5) \quad i_n = r_0 + c_n \cdot t ,$$

where r_0 – specific heat of water vaporization, kJ/kg ; c_n is the average specific heat capacity of water vapor, $\text{kJ}/(\text{kg.K})$.

The enthalpy of air entering the heater has been calculated and equals to 42.97 kJ/kg . The enthalpy of the air leaving the dryer is 122.87 kJ/kg .

Distribution of the difference in moisture content by zones, based on the moisture balance, in proportion to the amount of evaporated moisture in each zone [18]:

$$(6) \quad \Delta x_1 = \frac{x_2 - x_0}{W} \cdot W_1 ,$$

$\Delta x_1 = 3.07 \text{ g/kg}$; $\Delta x_2 = 6.15 \text{ g/kg}$; $\Delta x_3 = 6.15 \text{ g/kg}$; $\Delta x_4 = 5.13 \text{ g/kg}$. Moisture content at the exit and in further zones will be: $x_4 = 30.5 \text{ g/kg}$; $x_3 = 25.36 \text{ g/kg}$; $x_2 = 19.21 \text{ g/kg}$; $x_1 = 13.06 \text{ g/kg}$.

Specific consumption of completely dry air is calculated under the following formula:

$$(7) \quad l = \frac{1000}{x_2 - x_1} = 48,78 \text{ kg of air / kg of moisture},$$

where x_2 , x_1 – specific moisture content at the exit from the dryer and at the entrance to the heater.

Then total consumption of absolutely dry air in the drying unit

$$(8) \quad L = l \cdot W = 26593.17 \text{ kg/h} \quad 26593,17 \text{ kg/year} \quad (8)$$

Specific volume of moist air entering and leaving the drying chamber is calculated using formula [18]

$$(9) \quad \vartheta_{yA} = \frac{R_B \cdot T}{B - \phi P_h} ,$$

where K_B is the gas constant; T is absolute air temperature, K:

$$\vartheta_{yA1} = 0,85 \text{ m}^3/\text{kg}, \quad \vartheta_{yA2} = 0,96 \text{ m}^3/\text{kg}.$$

Volume consumption of air is determined using the formula

$$(10) \quad V = L \cdot \vartheta_{yA} ,$$

$$V_0 = 22604.19 \text{ m}^3/\text{h}, \quad V_2 = 25529.44 \text{ m}^3/\text{h}.$$

Let's determine the working length of the belt [18]

$$(11) \quad S = \frac{G_k \cdot \tau_1}{P_h \cdot f} ,$$

where τ_1 means drying time on the 1st belt, according to experimental data $\tau_1 = 25 \text{ min}$; P_h is the bulk density of dried material, kg/m^3 ; $P_h = 650 \text{ kg/m}^3$; f – cross-sectional area of dried material on the belt: $f = b \cdot h = 0,175 \text{ m}^2$; b – layer width: $b = 0,9 \cdot B_s - 0,05 = 1,75 \text{ m}$; (B_s is the width of the conveyor belt, according to the standard we assume $B_s = 2 \text{ m}$); h – the height of the lower belt's material $h = 36 \text{ mm}$; $S = 2.76 \text{ m}$. We assume 2.8 m .

Other belts have the same length. The working area of the drying unit's all belts is 19.6 m^2 for the belt's total working length of 11.2 m . The belt's width is 2000 mm .

Let's calculate the speed of the belts

$$(12) \quad v_1 = v_2 = v_3 = \frac{S}{\tau} = 0,11 \text{ m/s.}$$

The drying chamber's length

$$(13) \quad l_k = S_0 + d + r = 3,8 \text{ m},$$

where S_0 is the distance between the centers of the drums, which is equal to the working length of the belt; d – drum diameter; r – the belts' displacement relative to each other and the drums' distance to the walls of the drying chamber (we assume $r = 0.7 \text{ m}$).

Given the belt's width and the distance from the belt to the chamber's wall, we determine the chamber's width:

$$(14) \quad b_k = B_s + 2,0 \cdot 0,05 = 2,1 \text{ m.}$$

When calculating the chamber's height h between the drums, the distance between the drum and the ceiling is 0.234 m, and the distance between the drum and the floor is 0.3 m $h_k \approx 2,3 \text{ m.}$

Let us perform the calculation for the drying chamber with subsequent heat distribution across the dryer zones.

And let's calculate specific heat consumption for heating the material in the drying chamber [18]

$$(15) \quad q_m = \frac{G_k \cdot c''_m (\theta_2 - \theta_1)}{W}$$

where c''_m is specific heat capacity of dried material

$$(16) \quad c''_m = \frac{c_w \cdot \omega_2 + c_m (100 - \omega_2)}{100} = 1,49 \text{ kJ/kg·K}$$

c_w – specific heat capacity of water, $c_w = 4,19 \text{ kJ/kg·K}$; c_m – specific heat capacity of absolutely dry material; $C_m = 1,286 \text{ kJ/kg·K}$; θ_1 is the material's temperature at the entrance to the drying chamber, $\theta_1 = 117,6^\circ\text{C}$; θ_2 is the material's temperature at the exit from the drying chamber, $\theta_2 = 48^\circ\text{C}$. Average air temperature in the dryer

$$(17) \quad t_{cp} = \frac{t_1 + t_2 + t_3 + t_4}{4} = 57,27^\circ\text{C}.$$

Average temperature difference

$$(18) \quad \Delta t_{cp} = t_{cp} - t_h = 39,65^\circ\text{C}.$$

The chamber's equivalent diameter in the direction of air flow is determined from the following equation

$$(19) \quad d_s = \frac{2b_k \cdot l_k}{b_k + l_k} = 2,71 \text{ m}$$

The air movement velocity in the drying chamber is calculated based on the volumetric air flow V_2 according to the flow continuity equation:

$$(20) \quad \vartheta = \frac{V_2}{3600 \cdot f} = 1,8 \text{ m/s}$$

where f is the free cross-section for air passage in the chamber, taking into account the chamber's filling with material.

$$(21) \quad f = b_k \cdot l_k = 7,98 \text{ m}^2$$

We assume the free cross-section for air passage as equal to $0.5f$.

Let's calculate the Reynold's number [18, 19]:

$$(22) \quad Re = \frac{\vartheta \cdot d_s}{v} = 252419$$

where v is the kinematic viscosity of air at an average temperature.

Let's determine the heat transfer coefficient α'_1 [18]:

$$Nu = 0,32 \cdot Re^{0,8} = 671,0;$$

$$\alpha'_1 = Nu \cdot \lambda / d_e = 6,88 \text{ W/(m·K)};$$

where λ is the air thermal conductivity coefficient at an average temperature.

Let us calculate heat transfer coefficient α''_1 using equation [18, 20]

$$(23) \quad Nu = 0,15(GrPr)^{0,33}$$

where Pr is the Prandtl number [18-20]

$$(24) \quad Pr = \frac{v}{a}$$

Gr is Grashof's number [18]

$$(25) \quad Gr = \frac{g \cdot h_k^3}{v^2} \cdot \left(\frac{T_{cp} - T_{ct,b}}{T_{cp}} \right)$$

where a is the temperature conductivity coefficient of near-wall air, m^2/s ; g – free fall acceleration, m^2/s^2 ; T_{cp} is the absolute average air temperature, K.

We assume the wall's inner surface temperature as: $T_{ct,b} = 320 \text{ K}$.

The values of kinematic viscosity and air thermal conductivity coefficients are assumed at the following temperatures:

$$(26) \quad t = \frac{t_{cp} + t_{ct,b}}{2} = 52,13^\circ\text{C},$$

$$Pr = 0,73; Gr = 10,46; Nu = 273,85; \alpha'_1 = 3,26 \text{ W/(m·K)}$$

Heat transfer coefficient from air to the drying chamber's inner surface

$$(27) \quad \alpha_1 = A(\alpha'_1 + \alpha''_1) = 12,67 \text{ W/(m·K)}$$

where A is the coefficient depending on the air movement mode and the wall surface state.

Let's take the temperature of the wall's outer surface as $t_{ct,h} = 30^\circ\text{C}$, $t_h = 17,6^\circ\text{C}$. We will assume that the workshop's wall opposite to the dryer's wall has temperature: $t_{ct} = 17,6^\circ\text{C}$.

Air parameters are assumed at the average temperature $t_{h, cp} = 23,8^\circ\text{C}$.

Physical parameters of the air are taken at the average temperature:

$$(28) \quad t = \frac{t_{ct,h} + t_h}{2} = 23,8^\circ\text{C} \quad)$$

Grashof number according to formula (25)
 $Gr = 18,95 \cdot 10^9$.

Then from equation (23) the Nusselt number: $Nu = 334,62$; $\alpha''_2 = 3,7 \text{ W/(m·K)}$.

The coefficient of heat transfer from the drying chamber's outer surface to air α_2 is determined by heat losses due to air's natural convection in the room and to thermal radiation.

$$(29) \quad \alpha_2 = \alpha''_2 + \alpha_n$$

where α_n is the coefficient of heat transfer by thermal radiation, W/(m·K) [18]

$$(30) \quad \alpha_n = \frac{c_{1-2} \left[\left(\frac{T_{ct,h}}{100} \right)^4 - \left(\frac{T_{ct}}{100} \right)^4 \right]}{t_{ct,h} - t_h} = 4,34 \text{ W/(m·K)}$$

where c_{1-2} is thermal radiation coefficient,
 $\alpha_2 = 8,04 \text{ W/(m·K)}$.

The side and end walls of conveyor-type heat and mass exchange equipment and the door represent the panels assembled from two steel sheets with the thickness of $\delta_{st} = 1 \text{ mm}$. The space between the sheets is filled with an insulation layer (mineral wool) with the thickness of $\delta_i = 10 \text{ mm}$, $\lambda_{ct} = 45,4 \text{ W/(m·K)}$, $\lambda_u = 0,046 \text{ W/(m·K)}$.

The heat transfer coefficient for the side and end walls is calculated according to equation [18]:

$$(31) \quad k = \frac{1}{\frac{1}{\alpha_1} + \sum \frac{\delta_i}{\lambda_i} + \frac{1}{\alpha_2}} = 2,38 \text{ W/(m}^2\text{·K)})$$

Let's check the accepted temperatures of the dryer fence's outer and inner surfaces [18]:

$$t_{cr,H} = t_h + \frac{k\Delta t_{cp}}{\alpha_2} = 24,65 \text{ }^{\circ}\text{C};$$

$$t_{cr,B} = t_{cp} - \frac{k\Delta t_{cp}}{\alpha_1} = 42,34 \text{ }^{\circ}\text{C}.$$

Specific heat losses through side and end walls according to formula [18]

$$(32) \quad q_{cr} = 3,6 \frac{kF\Delta t_{cp}}{W} = 16,91 \text{ kJ/kg},$$

where F is the surface of the fence (walls, floors, ceilings), m^2 .

The surface of side and end walls:

$$F = 2(l_k \cdot h_k + b_k \cdot h_k) = 27,14 \text{ m}^2$$

Two exhaust chambers made of wood or metal are mounted in the upper part of the conveyor heat and mass exchange equipment. The insulation of the exhaust chambers and the ceiling is assumed the same as the dryer's walls. Based on the design of the exhaust chambers, the surface of the ceiling of conveyor-type heat and mass exchange equipment will be $9,17 \text{ m}^2$. Air temperature in the second zone is maintained at 45°C , then: $t_{average} = t_2 - t_0 = 41,4 \text{ }^{\circ}\text{C}$.

To simplify the calculation of the heat transfer coefficient, let us assume previously found heat transfer coefficients α_1 and α_2 changing them by 30%:

$$\alpha_1' = 2,28 \text{ W}/(\text{m}\cdot\text{K}), \alpha_2' = 3,038 \text{ W}/(\text{m}\cdot\text{K}).$$

Then, for the ceiling, the coefficient of heat transfer from air to the drying chamber's inner surface according to formula (27): $\alpha_1 = 11,45 \text{ W}/(\text{m}\cdot\text{K})$.

The coefficient of heat transfer from the drying chamber's outer surface to air according to formula (29): $\alpha_2 = 7,39 \text{ W}/(\text{m}\cdot\text{K})$.

The heat transfer coefficient is calculated according to equation (31): $k = 2,27 \text{ W}/(\text{m}^2\cdot\text{K})$.

Specific heat loss through the ceiling is calculated by formula (32): $q_{not} = 5,68 \text{ kJ/kg}$.

Specific heat losses through the floor are calculated according to the following formula [18]:

$$(33) \quad q_{not} = 3,6 \frac{kFq_{not}}{W} = 1,59 \text{ kJ/kg}$$

where F is the floor area, m^2 ; q_{not} is the specific heat loss from 1 m^2 of the floor, W/m^2 .

Total heat loss in the drying unit can be found using the following equation:

$$(34) \quad \Delta = (c_w \theta_1 + q_{don}) - (q_m + q_{tp} + q_{not}) = -13 \text{ kJ/kg}$$

where c_w is the specific heat capacity of water, $c_w = 4,19 \text{ kJ/kg}\cdot\text{K}$; θ_1 is the temperature of the material at the entrance to the drying chamber; q_{don} is the amount of heat that is additionally introduced into the drying chamber, kJ/kg ; q_m , q_{tp} is the specific heat consumption for heating the material and transport devices, respectively, kJ/kg ; q_{not} being the specific heat loss to the environment, kJ/kg .

Specific heat losses for material heating are referred to the second zone. This includes heat loss to the environment through the ceiling. The first zone includes heat loss through the floor. The heat introduced into the drying chamber with the material's moisture and lost to the environment through the side and end walls is distributed in proportion to the amount of moisture removed in each zone:

$$\Delta_4 = -54,23 \text{ kJ/kg}; \quad \Delta_3 = 17,05 \text{ kJ/kg}; \quad \Delta_2 = 17,05 \text{ kJ/kg};$$

$$\Delta_1 = 6,94 \text{ kJ/kg}.$$

We find the thermodynamic losses attributed to 1 kg of moisture according to the following formula:

$$(35) \quad q_{rep} = 0,23(T_1 + T_2),$$

where T_1 and T_2 mean the absolute air temperature at the entrance to the drying chamber and at its exit, respectively: $q_4 = 147,5 \text{ kJ/kg}$; $q_3 = 149,6 \text{ kJ/kg}$; $q_2 = 149,3 \text{ kJ/kg}$; $q_1 = 149,3 \text{ kJ/kg}$.

Taking into account the thermodynamic losses, the correction for real drying process in each zone will be as follows: $\Delta_4 = -201,73 \text{ kJ/kg}$; $\Delta_3 = -132,7 \text{ kJ/kg}$; $\Delta_2 = -132,4 \text{ kJ/kg}$; $\Delta_1 = -142,36 \text{ kJ/kg}$; $\sum \Delta = -608,99 \text{ kJ/kg}$.

Numerical simulation results

To evaluate the effectiveness of proposed structural and process flow diagram of the dryer and to check the adequacy of analytical calculations, we will perform the simulation of the drying process using Simcenter STAR-CCM+ software package and DEM (Discrete Element Method) method [21-23].

The DEM method is the numerical modeling method used to analyze the motion and interaction between particles. It is commonly used to study the behavior of granular materials such as sand, stone and grain, as well as to analyze processes occurring in various industries, such as oil and gas industry, food, agriculture, and pharmaceutical industries [24]. The DEM method models the movement of solid bodies that interact with each other through contact forces. To do this, each particle is represented separately and interactions between particles, such as impacts, friction and adhesion, are taken into account. Interaction parameters are defined for each pair of particles, on the basis of which the motion of each particle is calculated. The DEM method also takes into account the interaction between the particles and the environment, such as air or liquid. Application of the DEM method allows analyzing the behavior of granular materials and other types of discrete systems. It is a powerful tool for improving the efficiency and accuracy of designing processes related to the mixing, transfer and sorting of granular materials.

For simulation purposes, the 2D model of the area of heat and mass exchange equipment with belt conveyors moving in the horizontal plane was generated. Using the surface mesh generator and polyhedral cell generator with the linear size's reference value of 0.01 m, a three-dimensional mesh was generated for the area of the heat and mass exchange equipment (fig. 3).

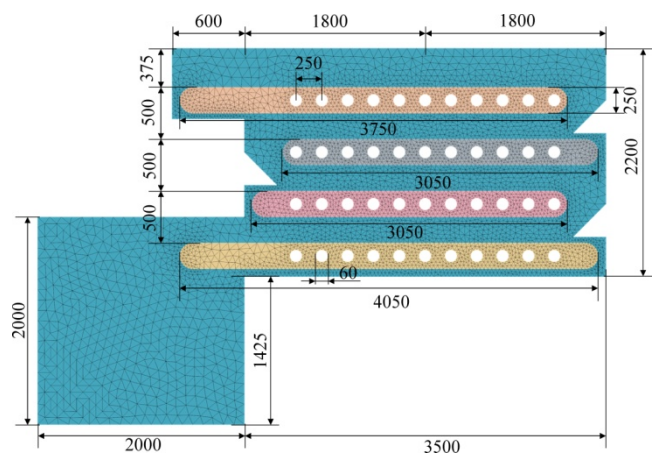


Fig. 3. Mesh of the area of heat and mass exchange equipment with belt conveyors

Next, we choose particular physical models in simulation. Selected models include the two-dimensional model, the unsteady implicit model, the one-component gas (air) mathematical model, the ideal gas (air) model, the turbulent air flow model, $k-\epsilon$ air turbulence model, the isothermal fluid energy equation, the averaged Navier-Stokes equation depending on the Reynolds number, the separated flow model, gradient and boundary methods, the Lagrangian model of multiphase medium, the multiphase interaction model, the discrete element model (DEM) and the gravity field [25-27].

Lucerne is represented as a Lagrangian phase according to the following models: the one of constant density, pressure gradient force, particles' resistive force, cylindrical particles, single-component solid particles and DEM particles. Lucerne had the following physical and mechanical properties: Poisson's ratio – 0.25; Young's modulus – 0.4 MPa; density – 500 kg/m^3 ; rest friction coefficient – 0.41; normal recovery factor – 0.35; tangent coefficient of recovery – 0.35; the coefficient of rolling resistance being 0.25. The following characteristics are assumed as geometric dimensions of lucerne: the average value of effective diameter – $D = 0.01 \text{ m}$; the average value of length is $L = 0.08 \text{ m}$; the minimum length value is $L_{\min} = 0.05 \text{ m}$; the maximum value of the effective length is $L_{\max} = 0.10 \text{ m}$; standard deviation – $\sigma_L = 0.02 \text{ m}$. The distribution of lucerne length is subject to normal distribution.

The interaction between lucerne particles was subject to the Hertz-Mindlin contact interaction model [28, 29]: the coefficient of rest friction is 0.41; normal recovery factor – 0.35; the tangent coefficient of recovery being 0.35.

The following parameters were taken as the properties of the environment [27, 30]: environment – air; dynamic viscosity – $1.85508 \cdot 10^{-5} \text{ Pa}\cdot\text{s}$; turbulent Prandtl number – 0.9; free fall acceleration – 9.8 m/s^2 ; pressure – 101325 Pa . The incoming air flow temperature is 60°C , the ambient temperature being 20°C .

Lucerne is loaded into the dryer using the upper belt conveyor based on the Lagrangian phase injection function with the following parameters: particle appearance probability – 0.8, initial particle velocity – 0 m/s and lucerne feed $Q = 81.77 \text{ kg/h}$. The belts' speed is 0.11 m/s. Air flow parameters corresponded to previous analytical calculations. The boundary conditions for the simulation are as follows. The interaction between lucerne particles and the dryer's walls obeyed the Hertz-Mindlin contact interaction model: the rest friction coefficient is 0.41; the normal recovery factor – 0.35; and the tangent coefficient of recovery being 0.35. The belt surface is opaque to lucerne particles and transparent to air flow. Total simulation time is 600 s. The number of iterations is 10. The simulation time step is 0.01 s.

Based on the simulation results, the visualization of air flow velocity distribution in the area of conveyor-type heat and mass exchange equipment was obtained in vector and scalar forms (fig. 4).

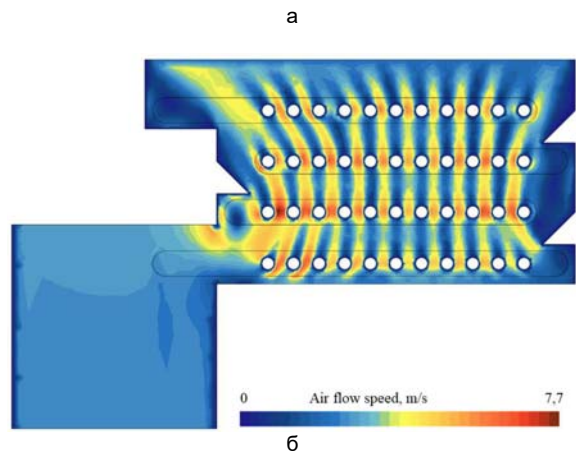
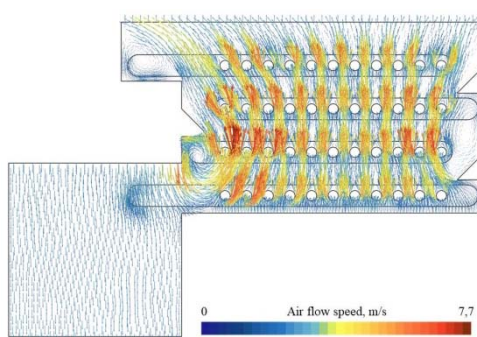


Fig. 4. Visualization of air flow velocity distribution in the area of conveyor-type heat and mass exchange equipment in vector (a) and scalar (b) forms

It follows from Fig. 4 that air flow bypasses the radiators. At the same time, the flow speed increases from 1.8 m/s at In the process of movement, the speed of relocation of fractionally processed leguminous grass products along the belt conveyors also changes. Respective visualization is shown in Fig. 5. On the belt, lucerne particles move at the uniform speed of 0.11 m/s, and in the process of their unloading from the belts, the speed increases due to free fall acceleration.

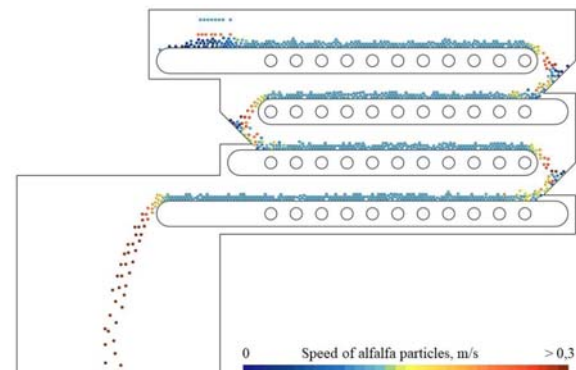


Fig. 5. Visualization of lucerne particles' flow rate distribution in the area of conveyor-type heat and mass exchange equipment in scalar form

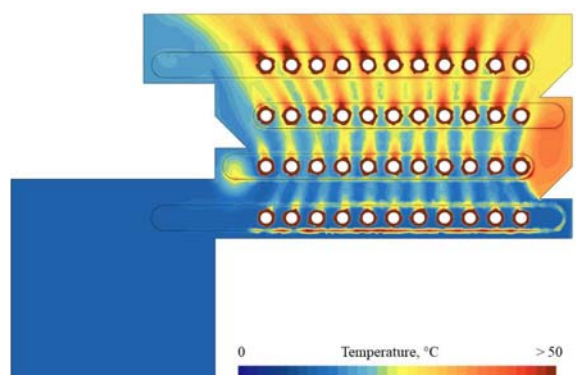


Fig. 6. Visualization of air flow temperature distribution in the area of conveyor-type heat and mass exchange equipment in scalar form

Let us consider the visualization of the process of air's heat and mass transfer during its heating by heaters (Fig. 6). It can be seen from Fig. 6 that air flow gradually heats up when passing through each level of heaters. Therefore,

the upper belt's lucerne will have a higher temperature than that on the lower one. This is confirmed by Fig. 7.

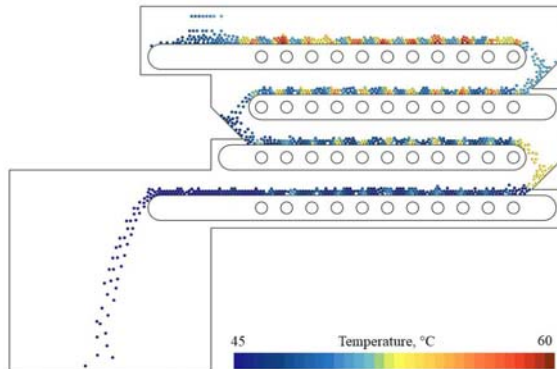


Fig. 7. Visualization of temperature distribution of lucerne particles' flow in the area of the conveyor-type heat and mass exchange equipment in scalar form

Presented numerical modeling results confirm the analytical calculations. However, in the future, it would be necessary to carry out experimental studies of the process of drying of legume grasses' fractional processing products and empirically to check rational structural-and-technological parameters of conveyor-type heat and mass exchange equipment.

Conclusions

Based on the results of research, the technological and constructive-technological scheme of the conveyor heat-mass exchange equipment for the fractional processing of leguminous herbs is substantiated, which is made in the form of a chamber with horizontal belt conveyors installed in it, in the middle of which are placed calorifiers with heated steam, and centrifugal fans are installed on top of the chamber.

Based on the results of analytical studies, the design and technological parameters of the developed conveyor heat-mass exchange equipment for the fractional processing of legumes were calculated. It was established that the productivity of the wet product is 1300 kg/h. The product comes out of the dryer at a humidity of 7% and a temperature of 45 °C. Based on the results of the calculation, we obtained the design parameters of the working area of the conveyor heat and mass exchange equipment: length – 3.8 m, width – 2.1 m and height 2.3 m. Total heat loss in the drying unit – 13 kJ/kg. The speed of the belt conveyor is 0.11 m/s.

Using the Simcenter STAR-CCM+ software package, a simulation of the technological process of drying in the developed conveyor heat and mass exchange equipment was carried out. Visualizations of the flow rate distribution of particles of products of fractional processing of legumes and air flow in the area of the conveyor heat and mass exchange equipment were obtained in scalar and vector form. The temperature distribution of the air flow in the area of the conveyor heat and mass exchange equipment was determined in a scalar form and its influence on the temperature of the particles of the fractional processing of leguminous grasses moving along belt conveyors was revealed.

The presented results of numerical modeling confirm the analytical calculations. However, in the future, it is necessary to carry out experimental studies of the drying process of products of fractional processing of leguminous herbs and empirically check the rational structural and technological parameters of the conveyor heat and mass exchange equipment.

Authors: KALETKI Hryhorii – Dr. Sc. in Economics, Professor, Academician NAAS of Ukraine, Head of the Department of Administrative Management and Alternative Fuel Resources, Vinnytsia National Agrarian University (21008, 3 Sonyachna str., Vinnytsia, Ukraine); YAROPUD Vitalii – PhD in Engineering, Associate Professor, Dean of the Faculty of Engineering and Technology, Vinnytsia National Agrarian University (21008, 3 Sonyachna str., Vinnytsia, Ukraine, e-mail: yaropud77@gmail.com); POLIEVODA Yurii – PhD in Engineering, Associate Professor, Faculty of Engineering and Technology, Vinnytsia National Agrarian University (21008, 3 Sonyachna str., Vinnytsia, Ukraine, e-mail: vinyura36@gmail.com); SOLONA Olena – PhD in Engineering, Associate Professor, Faculty of Engineering and Technology, Vinnytsia National Agrarian University (21008, 3 Sonyachna str., Vinnytsia, Ukraine, e-mail: solona_o_v@ukr.net); BABYN Ihor – PhD in Engineering, Associate Professor, Faculty of Engineering and Technology, Vinnytsia National Agrarian University (21008, 3 Sonyachna str., Vinnytsia, Ukraine, e-mail:igor_tverdokhlib@yahoo.com).

REFERENCES

- [1] Aliev, E.B., Mykolenko, S.Yu., Sova, N.A., and others. (2022). Technical and technological support of waste-free processing of grain raw materials into food products and fodder: collective monograph. LIRA. 192 p. ISBN 978-966-981-687-0.
- [2] Honcharuk I., Tokarchuk D., Gontaruk Y., Hreshchuk H. (2023). Bioenergy recycling of household solid waste as a direction for ensuring sustainable development of rural areas. *Polityka Energetyczna – Energy Policy Journal*. Vol. 26, Iss. 1. P. 23–42. <https://doi.org/10.33223/epj/161467>.
- [3] Honcharuk I., Yemchyk T., Tokarchuk D., Bondarenko V. (2023). The Role of Bioenergy Utilization of Wastewater in Achieving Sustainable Development Goals for Ukraine. *European Journal of Sustainable Development*. Vol. 12, No. 2. P. 231-244. <https://doi.org/10.14207/ejsd.2023.v12n2p231>
- [4] Mostovenko V., Mazur O., Didur I., Kupchuk I., Voloshyna O., Mazur O. (2022). Garden pea yield and its quality indicators depending on the technological methods of growing in conditions of Vinnytsia region. *Acta Fytotechnica et Zootecnica*. Vol. 25, № 3. P. 226-241. <https://doi.org/10.15414/afz.2022.25.03.226-241>
- [5] Mazur O., Kupchuk I., Voloshyna O., Matviiets V., Matviiets N., Mazur O. (2023). Genetic determination of elements of the soybean yield structure and combining ability of hybridization components. *Acta Fytotechnica et Zootecnica*. Vol. 26, № 2. P. 163-178. DOI: <https://doi.org/10.15414/afz.2023.26.02.163-178>
- [6] Xianzhe Z., Lan Y., Jianying W., Hangfei D. (2009). Process analysis for an alfalfa rotary dryer using an improved dimensional analysis method. *International Journal of Agricultural and Biological Engineering*. 2 (3). P. 76–82. DOI: [10.3965/j.issn.1934-6344.2009.03.076-082](https://doi.org/10.3965/j.issn.1934-6344.2009.03.076-082)
- [7] Mulle C. J. C., Cruywagen C. W., Du Toi F. J., Both J. A. (2008). The drying rate and chemical composition of field and artificially dried lucerne hay. *South African Journal of Animal Science*. 38 (4). P. 350–354.
- [8] Gallego A., Hospido A., Moreira M. T., Feijoo G. (2011). Environmental assessment of dehydrated alfalfa production in Spain. *Resources, Conservation and Recycling*. 55 (11). P. 1005–1012. DOI: [10.1016/j.resconrec.2011.05.010](https://doi.org/10.1016/j.resconrec.2011.05.010)
- [9] Adapa P. K., Schoenau G. J., Tabil L. G., Arinze E. A., Singh A. K., Dalai A. K. Customized and value-added high quality alfalfa products: a new concept. *Agricultural Engineering International: CIGR Journal*. 2007. 9. P. 1–28.
- [10] Farhang A., Hosinpour A., Darvishi H., Khoshtaghaza M. H., Tavakoli Hashjin T. (2010). Accelerated drying of alfalfa (*Medicago sativa* L.) by microwave dryer. *Global Veterinaria*. 5 (3). P. 158–163.
- [11] Neresi M. A., Castagnarall D. D., Mesquital E. E., Zambom M. A., Souza L. C., Rabello de Oliveira P. S., Jobim C. C. (2010). Production of alfalfa hay under different drying methods. *Revista Brasileira de Zootecnia*. 39(8). P. 1676–1683. DOI: [10.1590/S1516-35982010000800008](https://doi.org/10.1590/S1516-35982010000800008)

- [12] Kic P. Effect of different air velocities on convective thin-layer drying of alfalfa for livestock feeding. *Agronomy Research*. 2017. 15(3): 737–744.
- [13] Paziuk V.M., Petrova Zh.O., Tokarchuk O.A., Yaropud V.M. (2019). Research of rational modes of drying rape seed. *INMATEH - Agricultural Engineering*. Vol. 58, № 2. P. 303-310.
- [14] Paziuk V.M., Liubin M.V., Yaropud V.M., Tokarchuk O.A., Tokarchuk D.M. Research on the rational regimes of wheat seeds drying. *INMATEH - Agricultural Engineering*. 2018. Vol. 56, № 3. P. 39–48.
- [15] Spirin A., Kupchuk I., Tverdokhlib I., Polievoda Y., Kovalova K., Dmytrenko V. (2022). Substantiation of modes of drying alfalfa pulp by active ventilation in a laboratory electric dryer. *Przegląd Elektrotechniczny*. 98 (5). P. 11–15. doi:10.15199/48.2022.05.02
- [16] Kuznietsova I., Bandura V., Paziuk V., Tokarchuk O., Kupchuk I. (2020). Application of the differential scanning calorimetry method in the study of the tomato fruits drying process. *Agraarteadus*. Vol. 31, №2. P. 173–180. https://doi.org/10.15159/jas.20.14
- [17] Vasilevskyi O.M., Sevastianov V.M., Ovchynnykov K.V., Didych V.M., Burlaka S.A. (2023). Accuracy of Potentiometric Methods for Measuring Ion Activity in Solutions. *Lecture Notes in Networks and Systems*. Vol. 447. P. 181-189. https://doi.org/10.1007/978-981-19-1607-6_16
- [18] Tkachenko S. Y., Spivak O. Yu. (2007). Drying processes and installations. Tutorial. VNTU. 76 p.
- [19] Kupchuk I., Burlaka S., Galushchak A., Yemchyk T., Galushchak D., Prysiazhniuk Y. (2022). Research of autonomous generator indicators with the dynamically changing component of a two-fuel mixture. *Polityka Energetyczna – Energy Policy Journal*. Vol. 25, Iss. 2. P. 147–162. https://doi.org/10.33223/epj/150746
- [20] Bandura V., Bezbah I., Kupchuk I., Fialkovska L. (2023). Innovative methods of drying rapeseeds using microwave energy. *Polityka Energetyczna – Energy Policy Journal*. Vol. 26, Iss. 2. P. 217–230. https://doi.org/10.33223/epj/163328
- [21] Aliiev E., Pavlenko S., Golub G., Bielka O. (2022). Research of mechanized process of organic waste composting. *Agraarteadus, Journal of Agricultural Science*. XXXIII (1). P. 21–32. DOI: 10.15159/jas.22.04
- [22] Kaletnik G.M., Yaropud V.M. (2021). Physico-mathematical model of the ventilation system for injecting clean air in livestock premises. *Technology, energy, transport of agricultural industry*, 114 №. 3. P. 4-15. https://doi.org/10.37128/2520-6168-2021-3-1
- [23] Yaropud V. (2021). Analytical study of the automatic ventilation system for the intake of polluted air from the pigsty. *Scientific horizons*, 24. №. 3. P. 19-27. https://doi.org/10.48077/scihor.24(3).2021.19-27
- [24] Hraniak V. F., Matviychuk V. A., Kupchuk I. M. Mathematical model and practical implementation of transformer oil humidity sensor. *Electronics*. 2022. № 1 (26). P. 3-8. https://doi.org/10.53314/ELS2226003H
- [25] Yaropud V., Honcharuk I., Datsiuk D., Aliiev E. (2022). The model for random packaging of small-seeded crops' seeds in the reservoir of selection seeders sowing unit. *Agraarteadus, Journal of Agricultural Science*. XXXIII (1): 199–208. DOI: 10.15159/jas.22.08
- [26] Shevchenko I., Aliiev E. (2020). Improving the efficiency of the process of continuous flowmixing of bulkcomponents. *Eastern-European Journal of Enterprise Technologies*. 6/1 (108). P. 6-13. DOI: 10.15587/1729-4061.2020.216409
- [27] Kaletnik G.M., Yaropud V.M. (2022). Simulation of the heat and mass transfer process of the indirect-evaporative type heat exchanger. *Technology, energy, transport of agricultural industry*, 116. № 1. P. 4-15. https://doi.org/10.37128/2520-6168-2022-1-1
- [28] Wallin S. (2000) Engineering turbulence modeling for CFD with a focus on explicit algebraic Reynoldce stress models. *Doctoral thesis. Norsteds truckeri, Stockholm, Sweden*. 124 p.
- [29] Yaropud V., Kupchuk I., Burlaka S., Poberezhets J., Babyn I. (2022). Experimental studies of design-and-technological parameters of heat exchanger. *Przegląd Elektrotechniczny*. Vol. 98, № 10. P. 57-60 https://doi.org/10.15199/48.2022.10.10
- [30] Gunko I., Hraniak V., Yaropud V., Kupchuk I., Rutkevych V. (2021). Optical sensor of harmful air impurity concentration. *Przegląd Elektrotechniczny*. 97, № 7. P. 76-79. https://doi.org/10.15199/48.2021.07.15